J Mater Sci (2009) 44:2977–2984
DOI 10.1007/s10853-009-3395-x

Preparation and investigation of PVDF/PMMA/TiO_2 composite film

Wei Li · Hong Li · Yong-Ming Zhang

Received: 1 January 2009 / Accepted: 12 March 2009 / Published online: 2 April 2009

Abstract Polyvinylidene fluoride (PVDF)/Polymethylmethacrylate (PMMA)/Titanium dioxide (TiO_2) composite, and its films was prepared and studied in detail. The structure, morphology, crystalline behavior, thermal, and mechanical properties of PVDF/PMMA/TiO_2 film were investigated through FT-IR/ATR, SEM, XRD, DSC, TGA, and Py-GC/MS, respectively. The results showed that the blended material and its film have favorable thermal and mechanical properties. The TiO_2 particles finely dispersed in the composite featured by crystalline regions of PVDF and homogeneous amorphous regions consisted of PVDF and PMMA, resulting in an advantageous properties and improvement of tensile strength and elongation at break of the PVDF/PMMA film. However, the TiO_2 can greatly narrow the thermally stable margin of PVDF in PVDF/PMMA/TiO_2 composite for at least 100 °C with catalysis decomposition effect.

Introduction

Fluoropolymer is a well-known class of polymers that presents excellent protecting properties, and is widely used as protective materials such as coating and protective films. Poly(vinylidene fluoride) (PVDF), for example, exhibits good stability to rigorous temperatures, UV exposition, aggressive chemical environments, and excellent mechanical properties [1]. These characteristics, in combination with its shiny appearance and resistance to graffiti [2], render it an interesting candidate as protective materials. However, the high cost has been a limitation for its widespread applications.

Today, polymer blending is a versatile and widely used method for optimizing the cost–performance balance and increasing the range of potential applications [3], especially for fluoropolymer. PVDF is often blended with amorphous polymers, among which Poly(methyl methacrylate)(PMMA) has been the most studied compatible polymer with PVDF owing to cost, optical properties, and performance advantages [4, 5]. Previous reports [6–11] have indicated that PVDF and PMMA are molecularly miscible in the amorphous state, and the blends have been studied extensively by thermal analysis [12, 13], Fourier transform IR (FTIR) spectroscopy [10], simultaneous DSC/FT-IR measurement [14, 15], and X-ray scattering [9, 16]. The properties of the blend are highly dependent on PMMA content; however, increasing the PMMA content results in an increase in the glass transition temperature and a decrease in the melting temperature of PVDF. Mechanical properties of PVDF such as impact strength [17] and tensile strength [18] also dramatically decrease along with the addition of PMMA. A composition containing 70% of PVDF and 30% of PMMA is found to have optimal physical and optical properties: gloss, hardness, and solvent resistance [19].

As we know, incorporating inorganic particles into polymer matrix is a practicable way to obtain advanced materials of composite [20]. In recent years, organic/inorganic composite materials have attracted considerable attention in both scientific and industrial circles, because they offer attractive potential for diversification and application of traditional polymeric materials [21]. As an inorganic material, TiO_2 has received the most attention because of its excellent properties: long-term stability,

W. Li · H. Li · Y.-M. Zhang (✉)
School of Chemistry and Chemical Technology, Shanghai Jiao Tong University, Shanghai 200240, China
e-mail: ymzsjtu@yahoo.com.cn

nontoxicity, and its resistance to discoloration under UV light. Cao et al. have proved that the incorporation of TiO_2 particles had strong effect on the performance of PVDF films [22]. Smillie and Lenges [23] disclosed the PVDF/PMMA composite as a protective film with TiO_2 as a pigment in a patent to vary the kind of the film and get opaque films. Therefore, in order to improve the performance of PVDF/PMMA film and broaden its application field, TiO_2 particles may be workable. However, there are few detailed investigations on the structure and property of PVDF/PMMA/TiO_2 composite film. Moreover, presence of TiO_2 may have strong negative effect on the thermal stability of PVDF/PMMA because of its catalytic decomposition character. Previous research has reported the effect of TiO_2 on the thermal stability of PEN [24], PIS [25], and PMMA [26], but its effect on PVDF in PVDF/PMMA blend still needs to be studied. In this article, PVDF/PMMA/TiO_2 composite films were prepared by melt-extrusion. The structure and property of PVDF/PMMA/TiO_2 composite films were investigated in detail. The catalytic role of TiO_2 on the decomposition of PVDF was also studied by Py-GC/MS.

Experimental

Materials

PVDF powder (FR902), was supplied by Shanghai 3F Ltd. China. PMMA resin (HR1000L) was obtained from Kuraray Co., Ltd. (Japan). Rutile TiO2 particle (primary diameter 260–300 nm) was purchased from Meidilin Nanometer Material Development Co. Ltd. (Gansu, China).

Film preparation

PVDF/PMMA/TiO_2 composite films containing 0, 2, 5, and 10 wt% TiO_2 particles were prepared via a Brabender single-screw extruder (PLD651, Germany), and the composition of PVDF/PMMA was fixed as 7:3 of weight ratio. Composite materials were first pelletized and then extruded into films. The extruding speed was 30 rpm, and the set temperature of the head section was around 240 °C. The thickness of the films was about 40 μm tested by thickness gauge.

Scanning electron microscopy (SEM) observation

The morphologies of the cross section of PVDF/PMMA and PVDF/PMMA/TiO_2 samples was observed using a scanning electron microscope (SEM, JSM-6360LV, Japan) with an accelerating voltage of 15 kV. The cross section was obtained by fracturing the sample in liquid nitrogen. It was then vacuum-dried, coated with gold particles, and attached to a sample holder with the aid of conductive copper tapes.

X-ray diffraction analysis

X-ray diffraction (XRD) analysis of the films was performed to disclose the crystalline phase of the films. XRD patterns of PVDF were recorded on a Rigaku D/max-2500B2/PCX system. The radiation source (Cu Kα X-ray) was operated at 40 kV and 200 mA, with the scanning angle over the range of 5–50° (2θ) and the scanning velocity of 4°/min at room temperature.

Infrared analysis (IR)

Attenuated total reflection (ATR)-infrared spectra were recorded using a FT-IR spectrophotometer (Bruker, Tensor 27), at the resolution of 1 cm^{-1}, number of scans = 32.

Thermal measurements

Thermogravimetric (TG) measurements were performed on TGA Q50 under nitrogen atmosphere to measure thermal stability of the materials. Samples of extruded neat PVDF and PMMA, as well as blend pellets were examined from 40 to 800 °C at a heating rate of 10 °C/min.

Differential scanning calorimetry (DSC) was used to study the thermal properties of the PVDF/PMMA/TiO_2 composites on the model STA-449C thermal analyzer (NETZSCH Company) under nitrogen atmosphere. Appropriate films sealed in aluminum pans were first melted to 200 °C (heating I), then cooled to −50 °C, and again reheated to the melting point (heating II), with both the heating and cooling rates set at 10 °C/min. Melting temperatures and enthalpies were determined at the maximum of the peaks and from the peak areas, respectively. The PVDF crystallinity X_c was evaluated by Eq. 1 [27]:

$$X_c = \frac{\Delta H_f / \phi}{\Delta H_f^*} \quad (1)$$

where $\Delta H_f^* = 104.5$ J/g [7] is the melting enthalpy for a 100% crystalline PVDF, ΔH_f the melting enthalpy of the mixtures measured in DSC, and $\phi$is the weight fraction of PVDF in PVDF/PMMA blends.

Py-GC-MS

The Py-GC-MS experiments were performed with a PY-2020 pyrolyzer coupled with GCMS-QP2010 equipped with a DB-5 capillary column (30-m length, 0.25-mm diameter, 0.25-mm film thickness). The GC oven was set to 40 °C for the first 3 min, then heated with a rate of 10 °C/min up to

280 °C and held for 25 min. Mass selective detector operating in the electron impact mode at 70 eV energy. The source and interface were held at 200 and 300 °C, respectively. The mass scanning range was 26–800 amu. The carrier gas used was helium at constant flow (0.8 mL/min). Polymer samples weighing 1–2 mg were flash pyrolyzed at 370, 410, and 500 °C.

Mechanical testing procedures

Before determining mechanical properties, samples were machined and given accurate dimensions in order to be tested in conformity with the standards specified in the different tests. Tensile strength and elongation at break point of the films were measured according to GB/T1040-92, using a universal mechanical tester (Instron, model 4301, UK) at room temperature (25 °C). The deformation rate was 25 mm/min, and the distance was 24 mm between grips. Five specimens were studied in each case and the results reported below pertain to averages.

Water absorption

Water absorption experiment was conducted according to ASTM D570-98. The dry weight before immersion, m_0, was used as the initial weight of the specimen. After immersing in a deionized water bath at 23 °C for 24 h, the specimen was removed from the water, gently wiped with soft absorbent paper, and weighed (m_i).Water absorption was calculated using Eq. 2:

$$\text{Water absorption } (\%) = 100 \times \frac{m_i - m_o}{m_o} \quad (2)$$

Results and discussion

Structure and morphology

In this section, FTIR-ATR (attenuated total reflection) spectra were employed to identify the chemical structure of PVDF/PMMA/TiO_2 composite films of various composition ratios. As shown in Fig. 1, PVDF polymer spectrum presents absorption peaks at 880, 840, 764, and 750 cm^{-1} according to literature data [28–30].The presence of the absorption band at 1729 cm^{-1}, ascribed to the stretching of the carbonyl group, suggests the existence of PMMA in the blend [31]. The bands at 2925 and 2957 cm^{-1}, attributed to $-CH_2$ stretching mode of PMMA, exhibits noticeable changes in position as well as intensity which varies with the content of TiO_2, probably due to the interaction between PMMA and TiO_2 [32]. On the other hand, it can be seen clearly that the intensity of the band at 765 cm^{-1} which is characteristic of α crystalline phase of PVDF

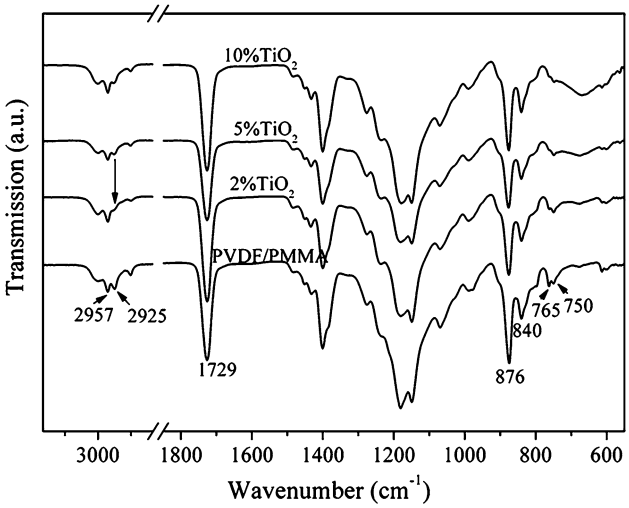

Fig. 1 FTIR spectra of PVDF/PMMA and its composites with different TiO_2 weight contents

deceases with the increase of TiO_2 content, implying the interaction between PVDF and TiO_2.

For organic/inorganic composite materials, dispersion level of inorganic particles in organic bulk is of great importance to the properties of composite materials. So microscopic investigation of the cross section of various composites was conducted using SEM. Figure 2 shows SEM micrographs of PVDF/PMMA (Fig. 2a) and its composites with different TiO_2 weight contents (Fig. 2b–d). We can see that during crystallization of PVDF/PMMA and PVDF/PMMA/TiO_2 from melt-extrusion, obvious phase separation is absent and cross section of each sample is characterized by a uniform pattern. Also, pristine TiO_2 particles disperse homogeneously in the polymer matrix at the content of 2–5 wt% as shown in Fig. 2b and c, as the TiO_2 content increases to 10 wt%, the film surface becomes rugged and the aggregates of particles are partially observed in Fig. 2d. Moreover, there is no aperture on the cross section, which indicates that all the films with different TiO_2 contents are dense and homogeneous.

Thermal properties

Thermal analyses using differential scanning calorimeter (DSC) and thermogravimetric (TGA) were performed in order to observe the effect of the addition of TiO_2 particles on the melting behavior and thermal stability of PVDF/PMMA film. The first and second run of the heating curves for films with different TiO_2 content are shown in Figs. 3 and 4, respectively. Thermal behavior of PVDF/PMMA/TiO_2 films with various weight ratios presents similar profile with that of PVDF/PMMA film, and peak shifts at melting and crystallization temperature are slight (Table 1). It is clear that irrespective of the TiO_2 content, the main

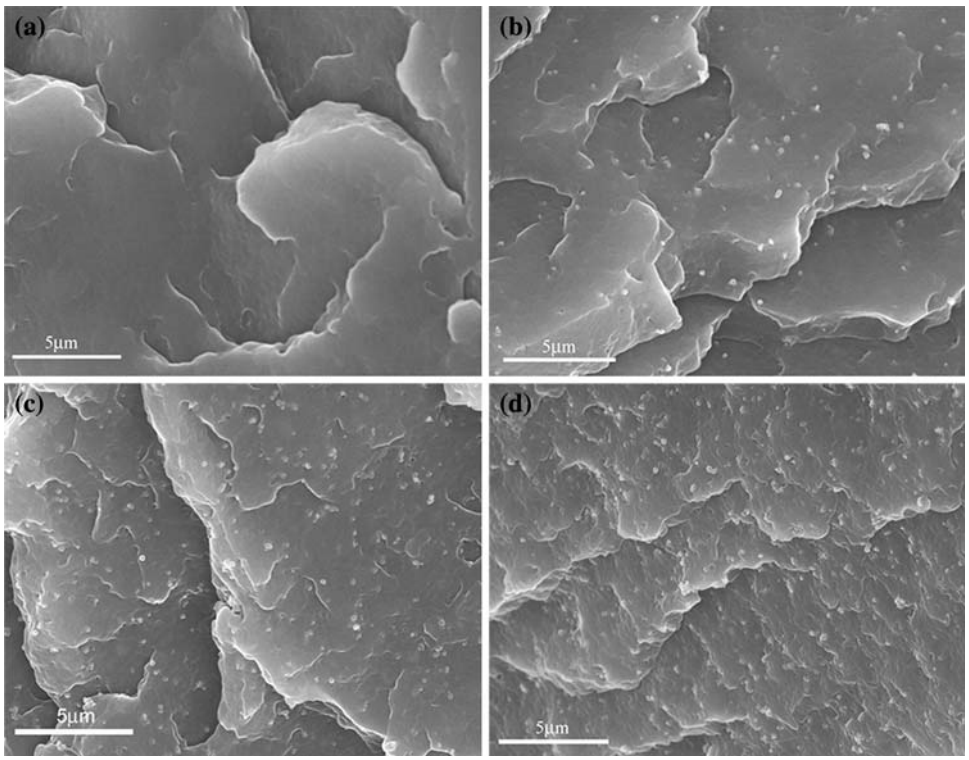

Fig. 2 The SEM micrograph of cross section of PVDF/PMMA blend (**a**) and PVDF/PMMA/TiO_2 blends: **b** 2 wt% TiO_2; **c** 5 wt% TiO_2; **d** 10 wt% TiO_2

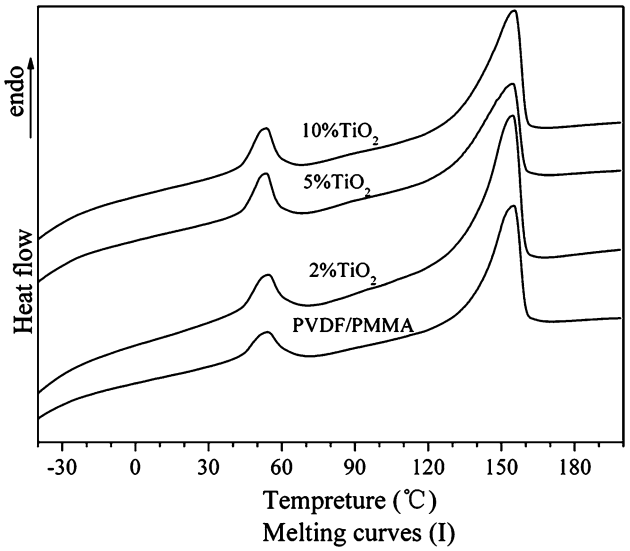

Fig. 3 DSC thermograms of PVDF/PMMA/TiO_2 with different TiO_2 weight contents at first (I) heating scan

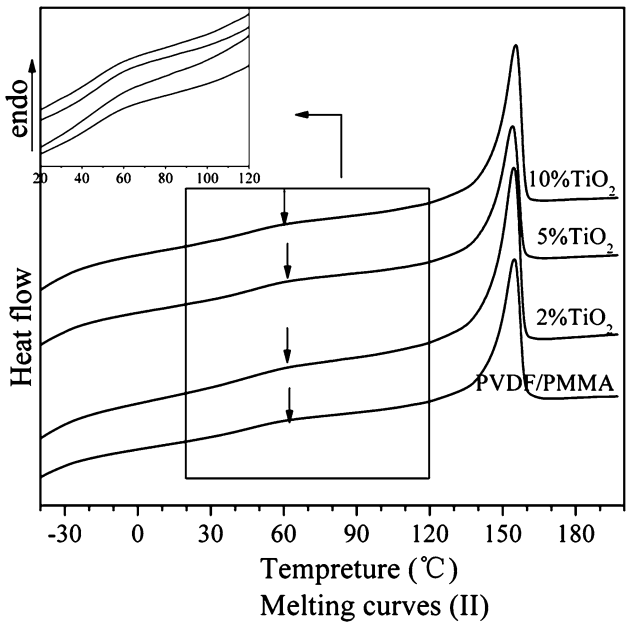

Fig. 4 DSC thermograms of PVDF/PMMA/TiO_2 with different TiO_2 weight contents at second (II) heating scan

endothermic peaks assigned to the melt points are almost same as 154–155 °C in the two heating curves.

Furthermore, it is noteworthy that all the samples present a small endothermic response around 50 °C in Fig. 3. Cebe and Chung [33] attributed this phenomena to both the rate of quenching through the glass transition and the length of time the samples were hold at room temperature before scanning. Amorphous blends show an "aging" peak when stored below their glass transition temperature. If the original cooling rate is less than the subsequent heating rate, an endothermic peak develops near the glass temperature [34]. However, after a cooling, the endotherm around 50 °C is greatly weakened in the second heating run. The very weak peak between 50 °C and 60 °C shown in Fig. 4 is assigned to the glass transition temperature of

Table 1 Thermal properties of PVDF/PMMA/TiO_2 composites

Samples	T_m^I (°C)	ΔH_m^I (J/g)	X_c (%)	T_c (°C)	T_m^{II} (°C)
PVDF/PMMA	155.22	26.08	35.65	124.46	154.81
2 wt% TiO_2	154.59	28.12	38.44	124.41	154.57
5 wt% TiO_2	154.62	26.17	35.78	122.48	154.12
10 wt% TiO_2	155.50	24.66	33.71	126.54	155.42

T_m Melting temperature, T_c Crystalline temperature, ^{I} The first heating, ^{II} The second heating

PVDF/PMMA composite according to early investigations [35], and it is rarely changed by the addition TiO_2.

TGA results of pure PVDF, PMMA pellets, and the composite materials are displayed in Fig. 5. The temperature at which the weight loss was 5% from its original weight is used as a weight loss "onset" temperature to evaluate the thermal stability. The onset temperatures of PVDF and PMMA are respectively 438 °C and 336 °C indicating the higher thermal stability of PVDF. The two-step weight loss of PVDF/PMMA blend which is proportional to the weight fraction of PMMA and PVDF is due to the individual degradation of PMMA and PVDF, respectively. Thermal stability of PMMA is enhanced by the presence of PVDF in PVDF/PMMA composite. With regard to the incorporation of TiO_2 particles, Fig. 5 indicates that the composites present lower thermal stability compared to the PVDF/PMMA blend, and the onset temperature decreases with the increase in the weight content of TiO_2 in the composites. The 10 wt% composite has an onset temperature of 327 °C, which decreases by about 32 °C, compared to that of PVDF/PMMA blend up to 359 °C. Although the composites are thermally stable above 300 °C, thermal degradation of PMMA chain would occur above 200 °C processing temperature [36], and so the processing temperature and extruding speed should be controlled to avoid the decomposition in film processing.

With regard to the residual portion, for temperatures between 500 and 800 °C, PMMA decomposes completely while PVDF has a high residual production of 26%. Residue of the composite increases with the TiO_2 weight. The composite with 2 wt% TiO_2 content has a 32% residue at 800 °C, compared to the 22% residue of PVDF/PMMA polymer. This might be occurring due to the decomposition paths of PVDF and PMMA. From the peaks given by Py-GC/MS in Fig. 6, it is indicated that HF is the major decomposition product of PVDF; HF formation further leads to the introduction of unsaturation in the polymer backbone which is difficult to decompose completely, resulting in a high amount of char in PVDF and PVDF/PMMA decomposition. Residual portion further increases after the introduction of TiO_2, which may be attributed to the reaction between the chelating ligands of titanium ion and the production of fluoride during backbone homolysis in the PVDF decomposition which could result in new products that are hard to decompose.

Moreover, PVDF/PMMA/TiO_2 composites present typical weight loss curves which only show one-step weight loss compared to the two-step weight loss of PVDF/PMMA blend, and the decomposition has a much higher speed than that of PVDF/PMMA blend. Since TiO_2 is very stable and no decomposition takes place below 600 °C [37], the possible reason for the decrease in thermal stability might be the presence of metal oxide-catalyzed oxidative decomposition pathways in the composite [38, 39], which is due to the catalytic effect of TiO_2 in the decomposition of PVDF and PMMA.

Py-GC/MS was employed to further analyze the catalytic effect of TiO_2 on the decomposition of PVDF/PMMA composite. Figure 6 displays Py-GC/MS results of PVDF/

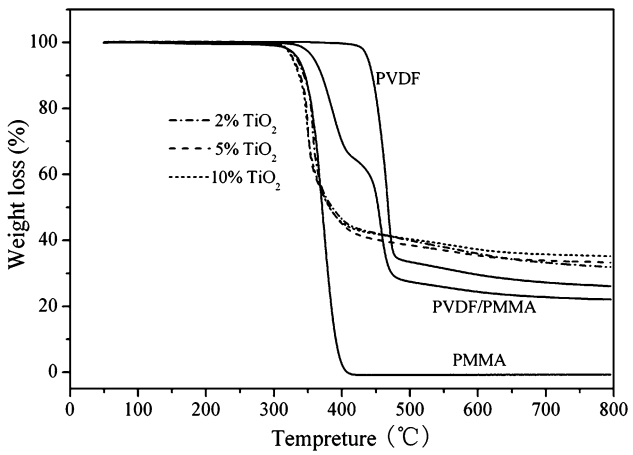

Fig. 5 TGA thermograms of PVDF, PMMA, and its composites with different TiO_2 weight contents

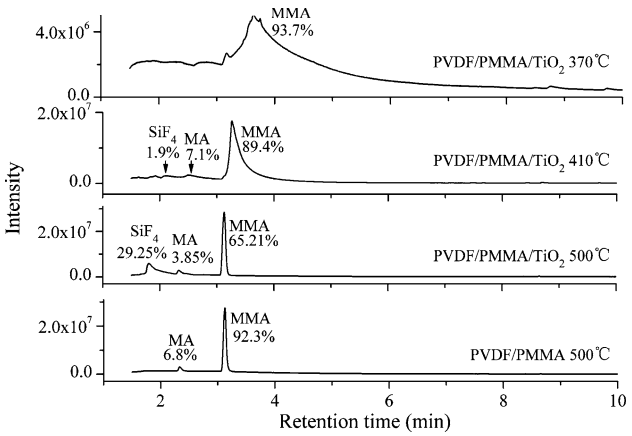

Fig. 6 Py-GC/MS results of PVDF/PMMA and PVDF/PMMA/TiO_2 composites results

PMMA and PVDF/PMMA/TiO_2 (5 wt% TiO_2) composites. The assignment of the peak and peak area is recorded next to the peak. For PVDF/PMMA/TiO_2 composite at the low temperature of 370 °C, only PMMA decomposes with MMA monomer (retention time between 3 and 5 min) as the major decomposition product (peak area: 97.3%). At the pyrolysis temperature of 410 °C, PVDF decomposes as indicated by the low amount of SiF_4. When the pyrolysis temperature reaches 500 °C, the main decomposition products of PVDF/PMMA/TiO_2 are not changed, butonly proportions vary with more HF product (29.25%). However, at this temperature, PVDF is still stable in PVDF/PMMA blend. The data suggest that addition of TiO_2 did not change the decomposition products of PVDF and PMMA. During decomposition of PVDF/PMMA/TiO_2, PMMA undergoes decomposition first followed by that of PVDF, but presence of TiO_2 significantly lowers the decomposition temperature of PVDF.

Crystalline property

Crystalline property of the composites can be indicated by X_c calculated from ΔH_m^I of DSC result in Table 1. After the incorporation of 2 wt% TiO_2, the crystallinity is enhanced, but it decreases along with the addition of TiO_2 particles. This could be attributed to the fact that at low loading level(2 wt%), TiO_2 acts as a nucleation site in the crystallization and promotes nucleation of PVDF crystalline phase, but at higher loading level, TiO_2 functions as filler and prevents rearrangement of PVDF macromolecular chain to form crystals [40]. This has been re-examined by the result of mechanical properties, which will be discussed later.

XRD was employed to further investigate the change in crystallinity due to the addition of TiO_2 particles in the PVDF/PMMA film. X-ray diffraction patterns of TiO_2, PVDF/PMMA blend and its composites with different TiO_2 weight contents are shown in Figs. 7 and 8, respectively. The characteristic peak at 27.55 in Fig. 7corresponds to (110) plane of the larger rutile TiO_2 particles. When the amount of TiO_2 increases in PVDF/PMMA composite, the intensity of the peak in 27.55° increases quickly as shown in Fig. 8.

It is well known that PVDF has two main crystal phrases, namely, α and β crystalline. As illustrated in Fig. 8, PVDF/PMMA film shows four main characteristic peaks, peaks at 2θ of 18.30, 19.90, and 26.56 are assigned to α crystalline, and 20.26 ascribed to β crystalline [41, 42]. Both α and β crystallines exist in PVDF/PMMA and PVDF/PMMA/TiO_2 composites, and the corresponding peaks all shift toward left or right, a little. When 2 wt% TiO_2 is added, the peak around 20° splits into two apparent peaks, but the presence of TiO_2 in PVDF/PMMA does not change the crystalline phase of PVDF.

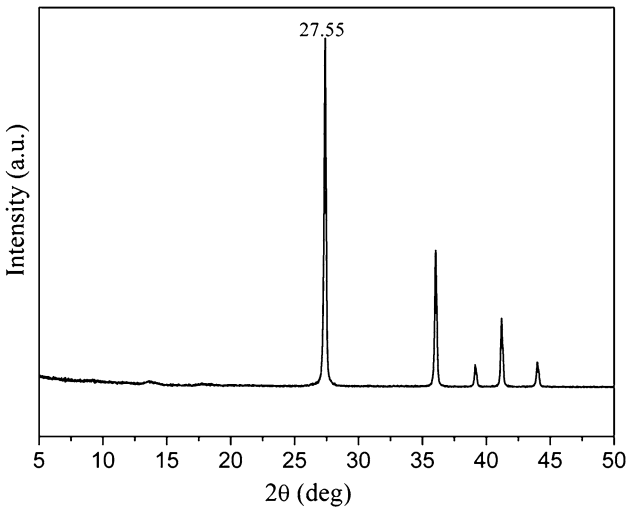

Fig. 7 X-ray diffraction pattern of TiO_2

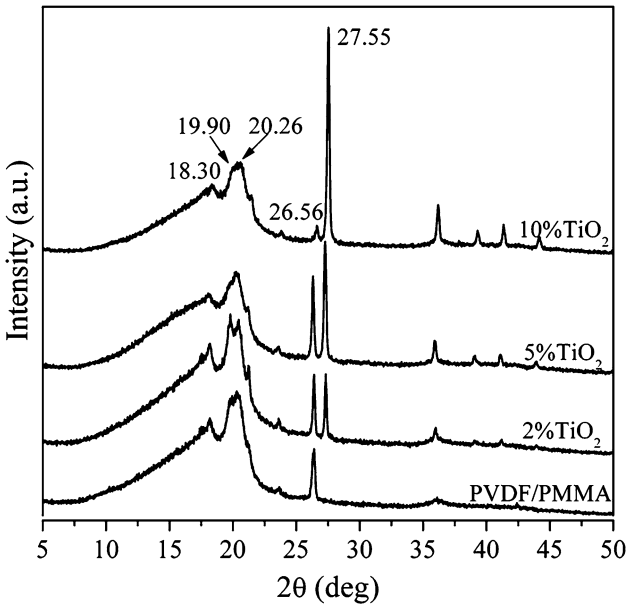

Fig. 8 X-ray diffraction patterns of PVDF/PMMA and its composites with different TiO_2 weight contents

Mechanical properties

The mechanical properties of the composite films such as tensile strength and elongation at break as a function of weight fraction of TiO_2 are displayed in Fig. 9. PVDF/PMMA film shows excellent mechanical properties as engineering plastics. Changes in mechanical properties are evident with increasing fraction of TiO_2 in the composite films. Introduction of TiO_2 particles increases the values of the tensile strength, and the increase of the elongation at break is more prominent. Compared to that of PVDF/PMMA blend, tensile strength of the film with 2 wt% of

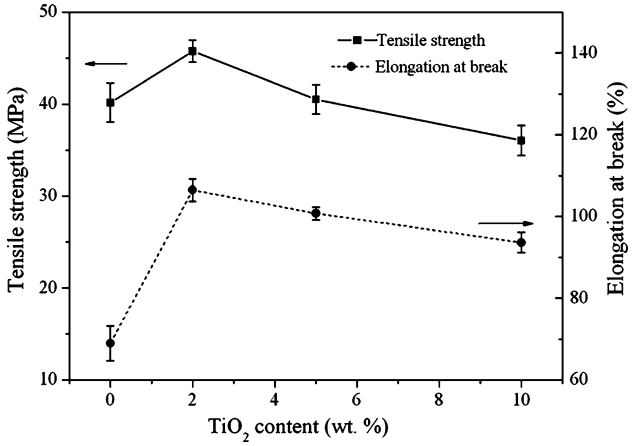

Fig. 9 Tensile strengths and elongations at break of PVDF/PMMA and its composites with different TiO_2 contents

TiO_2 increases by 12.67%, while the elongation at break increases by 54.41%.

For the tensile strength, there is an increase in the value from 0 to 2 wt% TiO_2 in the composite, followed by a decrease beyond 2 wt%. This result agrees well with that of the composite containing 2 wt% TiO_2 particles, which possesses an optimum level of dispersion seen from SEM image (Fig. 2) and the highest crystallinity (Table 1). When the additive TiO_2 reaches a certain critical value, tensile strength decreases because of the reduction of the crystallinity. Also, the increasing amount of TiO_2 particles makes it more difficult for dispersion, and easier for particles' "agglomeration". Since agglomerated particles make it possible to generate defects in the composites, stress concentration would likely occur within PVDF/PMMA, resulting in a decreased tensile strength.

With regard to the elongation at break, after the incorporation of TiO_2 particles, all the values are higher than that of PVDF/PMMA blend. Enhancement in the values is probably due to the fact that some TiO_2 particles functioned as physical junctions in the films during the drawing. The values decrease beyond 2 wt% along with the reduction of crystallinity, because film with lower crystallinity would break at a smaller stress, resulting in the decrease of the elongation at break.

Water absorption

Water absorption represents the value for water saturation. Organic polymeric materials will absorb moisture to some extent resulting in swelling, dissolving, leaching, plasticizing, and/or hydrolyzing, events which can result in discoloration, loss of mechanical and electrical properties, lower resistance to heat and weathering, and stress cracking. Therefore, for the protective films used in outdoor environment, low water absorption value is necessary. From the test results, we find that all the water absorption values of the composites films are below 0.1%, implying the low-moisture transmission.

Conclusion

The composite films of PVDF/PMMA/TiO_2 with favorable thermal and mechanical properties were prepared by melt-extrusion. Their structure and property were investigated in detail. Fine phase dispersions of TiO_2 particles in the composite were realized at TiO_2 low loading levels (2 and 5 wt%), and slight interactions occur among PVDF, PMMA, and TiO_2. As for thermal stability of the composite, the degradation temperature of the composite is still high, although the presence of TiO_2 catalyzes the decomposition of PVDF. Crystallinity of PVDF increases when 2 wt% of TiO_2 is added to the PVDF/PMMA system, which results in maximum value of the tensile strength and elongation at break of the PVDF/PMMA/TiO_2 composites (45.76 MPa, 106.42%). The films also show very low water absorption. Hence, all the results indicate that the addition of low content (2 wt%) TiO_2 particles can improve the mechanical properties of PVDF/PMMA film while basically maintaining its intrinsic good thermally stable properties. Considering the excellent comprehensive properties and good cost–performance balance, this kind of film has a promising future forapplication in industry.

Acknowledgement The authors acknowledge the grant of funds sanctioned for the "11th 5-year" National Key Technologies R&D Program (No. 2006BAE02A04) and Sino-Canada International Project (20073823).

References

1. Kirk-Othmer (1980) Encyclopedia of Chemical Technology. John Wiley & Sons Inc, USA
2. Bonnet A, Francois B, Karine L et al (2004) US Patent 6811,859
3. Liu ZH, Marechal P, Jerome R (1998) Polymer 39:1779–1785
4. Roerdrink E, Challa G (1978) Polymer 19:73
5. Iezzi RA (1997) In: Scheirs J (ed) Modern fluoropolymers. Wiley, New York
6. Noland JS, Hsu NNC, Saxon R et al (1971) Adv Chem Ser 99:15
7. Nakagawa K, Ishida Y (1973) J Polym Sci B Polym Phys 11:2153–2171
8. Nishi T, Wang TT (1975) Macromolecules 8:909
9. Paul DR, Altamirano JO (1975) Adv Chem Ser 142:371
10. Bernstein RE, Cruz CA, Paul DR et al (1977) Macromolecules 10:681
11. Huang C, Zhang L (2004) J Appl Polym Sci 92:1–5
12. Horibe H, Baba F (2000) Nippon Kagaku Kaishi, pp 115–120
13. Jarray J, Larbi FBC, Vanhulle F et al (2003) Macromolecular Symposia 198:103–116
14. Yoshida H (1997) J Therm Anal 49:101–105
15. Yoshida H, Zhang GZ, Kitamura T et al (2001) J Therm Anal Calorim 64:577–583
16. Hirata Y, Kotaka T (1981) Polym J 13:273

17. Mijovic J, Luo HL, Han CD (1982) Polym Eng Sci 22:234
18. Murff SR, Barlow JW, Paul DR (1986) Adv Chem Ser 211:313–324
19. Schneider S, Drujon X, Wittmann JC et al (2001) Polymer 42:8799–8806
20. Sun YP, Hao EC, Zhang X et al (1997) Langmuir 13:5168–5174
21. Pinnavaia TJ, Beall GW (2001) Polymer-clay nanocomposites. John Wiley and Sons, New York
22. Cao XC, Ma J, Shi XH et al (2006) Appl Surf Sci 253:2003–2010
23. Smillie BA, Lenges GM (2006) US No. 960,426:9
24. Li C, Tang AB, Zou YB et al (2005) Mater Lett 59:59–63
25. Liaw WC, Chen KP (2007) Eur Polym J 43:2265–2278
26. Laachachi A, Ferriol M, Cochez M et al (2008) Polym Degrad Stab 93:1131–1137
27. Gu MH, Zhang J, Wang XL et al (2006) J Appl Polym Sci 102:3714–3719
28. Bormashenko Y, Pogreb R, Stanevsky O et al (2004) Polym Test 23:791–796
29. Wang CL, Li JC, Zhong WL et al (2003) Synth Met 135:469–470
30. Kobayashi M, Tashiro K, Tadokoro H (1975) Macromolecules 8:158
31. Kazarian SG, Chan KLA (2004) Macromolecules 37:579–584
32. Ahmad S, Saxena TK, Ahmad S et al (2006) J Power Sources 159:205–209
33. Cebe P, Chung SY (1990) J Mater Sci 25:2367–2378. doi: 10.1007/BF00638031
34. Richardson MJ, Savill NG (1977) Polymer 18:413
35. Zhou XX, Cakmak M (2007) J Macromol Sci Phys 46:667–682
36. Gallagher GA, Jakeways R, Ward LM (1991) J Polym Sci B Polym Phys 29:1147
37. Feng W, Sun EH, Fujii A et al (2000) Bull Chem Soc Jpn 73:2627–2633
38. Sawada T, Ando S (1998) Chem Mater 10:3368–3378
39. Rancourt JD, Taylor LT (1987) Macromolecules 20:790–795
40. Kim BC, Choi CG, Han SP et al (2002) Polymer-Korea 26:462–467
41. Sajkiewicz P, Wasiak A, Goclowski Z (1999) Eur Polym J 35:1581–1590
42. Gregorio RJ, Cestari M (1994) J Polym Sci B Polym Phys 32:859